Severe Neonatal Hyperbilirubinemia in Crigler-Najjar Syndrome Model Mice Can Be Reversed With Zinc Protoporphyrin

Ryoichi Fujiwara,[1-3] Ryo Mitsugi,[3] Asuka Uemura,[3] Tomoo Itoh,[3] and Robert H. Tukey[4]

Neurotoxic bilirubin is solely conjugated by UDP-glucuronosyltransferase (UGT) 1A1. Due to an inadequate function of UGT1A1, human neonates develop mild to severe physiological hyperbilirubinemia. Accumulation of bilirubin in the brain leads to the onset of irreversible brain damage called kernicterus. Breastfeeding is one of the most significant factors that increase the risk of developing kernicterus in infants. Why does the most natural way of feeding increase the risk of brain damage or even death? This question leads to the hypothesis that breast milk-induced neonatal hyperbilirubinemia might bring certain benefits to the body. One of the barriers to answering the above question is the lack of animal models that display mild to severe neonatal hyperbilirubinemia. A mouse model that develops neonatal hyperbilirubinemia was previously developed by a knockout of the *Ugt1* locus. Deletion of *Ugt1a1* results in neonatal lethality from bilirubin neurotoxicity. Bilirubin is the end product of heme catabolism in which heme oxygenase-I is largely involved. When zinc protoporphyrin, an inhibitor of heme oxygenase I, was administered to newborn $Ugt1^{-/-}$ mice, serum bilirubin levels dropped dramatically, rescuing the mice from bilirubin-induced neonatal lethality. Zinc protoporphyrin-treated $Ugt1^{-/-}$ mice developed normally as adults capable of reproducing, but their newborns showed even more severe hyperbilirubinemia. Microarray analysis of the hyperbilirubinemic livers indicated that a number of genes associated with nucleotide, transport, and immune response were significantly down-regulated in a serum bilirubin level-dependent manner. *Conclusion*: Our study provides an opportunity to advance the development of effective therapeutics to effectively and rapidly prevent bilirubin-induced toxicity. Neonatal hyperbilirubinemia has various impacts on the body that could be driven by the antioxidant property of bilirubin. (*Hepatology Communications* 2017;1:792–802)

Introduction

Newborn children's breathing and excessive oxygen intake stimulates red blood cell hemolysis. Heme is a porphyrin that is coordinated with Fe(II) and is the oxygen-carrying portion of hemoglobin in red blood cells. Hemolysis results in the release of hemoglobin and heme from red blood cells. The reticuloendothelial system participates in oxidative degradation of heme by heme oxygenase-I (HO-I) to form biliverdin,[1] which is immediately reduced to bilirubin by bilirubin reductase (Fig. 1).[2]

Abbreviations: cDNA, complementary DNA; CN, Crigler-Najjar syndrome; CNS, central nervous system; CYP, cytochrome P450; GO, gene ontology; HO-I, heme oxygenase-I; hUGT1, humanized UGT1; KO, knockout; NAFLD, nonalcoholic fatty liver disease; PP, protoporphyrin; SNH, severe neonatal hyperbilirubinemia; TSB, total serum bilirubin; UGT, UDP-glucuronosyltransferase; ZnPP, zinc protoporphyrin..

Received June 2, 2017; accepted July 20, 2017.

Additional Supporting Information may be found at onlinelibrary.wiley.com/doi/10.1002/hep4.1082/full.

Supported by the Institutional Strategy of the University of Tübingen, Germany (Deutsche Forschungsgemeinschaft, ZUK 63 to R.F.). Funding for this work was also provided in part by a grant-in-aid for Encouragement of Young Scientists (B 26870562 to R.F.), grants-in-aid for scientific research from the Ministry of Education, Science, and Culture of Japan (15K09710 to R.F.), and in part by U.S. Public Health Service Grants P42ES010337 and GM086713 to R.H.T.

View this article online at wileyonlinelibrary.com.

DOI 10.1002/hep4.1082

Potential conflict of interest: Nothing to report.

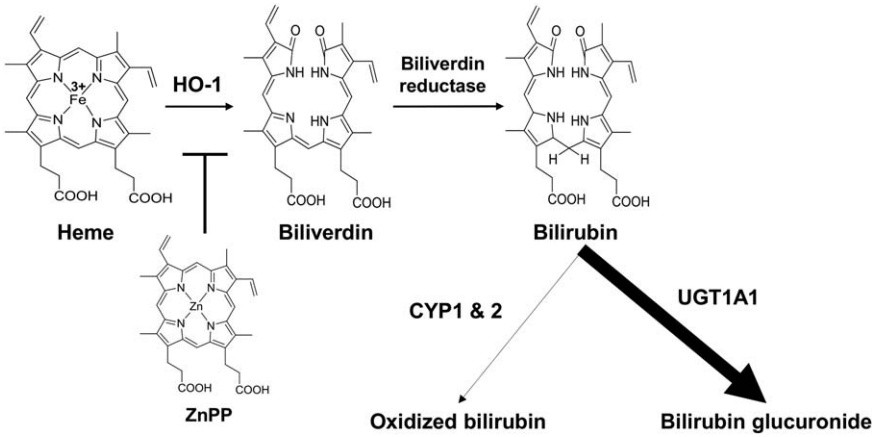

FIG. 1. Generation and metabolism of bilirubin. HO-1 mainly contributes to the catabolism of heme, producing biliverdin. Biliverdin reductase converts biliverdin into bilirubin. Bilirubin is mainly metabolized by UGT1A1 but is partially metabolized by CYP enzymes. Genetic deficiency in *UGT1A1* results in the onset of severe hyperbilirubinemia, which leads to the development of kernicterus.

Whereas biliverdin is hydrophilic and nontoxic, bilirubin is highly hydrophobic and neurotoxic.[3] In mammals, bilirubin is mainly detoxified by UDP-glucuronosyltransferase (UGT) 1A1, which mediates the glucuronidation of bilirubin to form hydrophilic and nontoxic mono- and di-glucuronides.[4] In addition, bilirubin can be subject to partial metabolism by cytochrome P450s (CYPs), which form oxidized metabolites.[5]

Newborn children develop mild hyperbilirubinemia, called jaundice, due to inadequate expression of UGT1A1 in the liver and small intestine.[6] Because total serum bilirubin (TSB) levels often fall without additional treatment within several weeks after birth, such conditions are physiological. In contrast, genetic deficiencies that leave the *UGT1A1* gene defective cause severe neonatal hyperbilirubinemia (SNH). Crigler-Najjar syndrome type I (CN-I) and type II (CN-II) are inherited diseases in which *UGT1A1* is completely or severely deficient, respectively.[7] Whereas CN-II can be treated by chemical induction of the *UGT1A1* gene by agents such as phenobarbital, the treatment for CN-I is more complex and often requires transplantation of the liver or hepatocytes. The extremely high TSB levels in CN-I lead to filtration of bilirubin into brain tissue. Due to the neurotoxic property of bilirubin, its accumulation in brain tissue can lead to acute bilirubin encephalopathy, followed by the more chronic form called kernicterus.[8] Although there are examples of patients with CN-I who have reached adulthood without requiring a liver transplant, the syndrome is often lethal if immediate and drastic clinical intervention is not available. The current therapies to interrupt the steady increase in SNH, such as extensive phototherapy, exchange transfusion, or liver transplant, are designed to eliminate bilirubin after its accumulation. An alternative approach is to prevent the accumulation of bilirubin. To examine this possibility, animal models with deficiencies in UGT1A1 expression can be used to develop new tools aimed at preventing bilirubin accumulation.

When the mouse *Ugt1a1* gene and the *Ugt1* locus are rendered inactive in *Ugt1*$^{-/-}$ mice, newborn *Ugt1*$^{-/-}$ mice develop SNH composed of unconjugated bilirubin, resulting in accumulation of bilirubin

ARTICLE INFORMATION:

From the [1]Dr. Margarete Fischer-Bosch Institute of Clinical Pharmacology, Stuttgart, Germany; [2]Department of Biochemistry and Pharmacy, University of Tübingen, Tübingen, Germany; [3]Department of Pharmaceutics, School of Pharmacy, Kitasato University, Tokyo, Japan; [4]Laboratory of Environmental Toxicology, Department of Pharmacology, University of California San Diego, La Jolla, CA.

ADDRESS CORRESPONDENCE AND REPRINT REQUESTS TO:

Ryoichi Fujiwara, Ph.D.
Dr. Margarete Fischer-Bosch Institute of Clinical Pharmacology
and University of Tübingen, Auerbachstr. 112
Stuttgart 70376, Germany

E-mail: ryoichi.fujiwara@ikp-stuttgart.de
or fujiwarar@pharm.kitasato-u.ac.jp
Tel: + 49-(0)711-8101-5002

in the brain and lethality within 1-2 weeks after birth.[9] Disruption of the *Ugt1* locus generated a phenotype that resembles CN-I disease. It was subsequently shown that the lethality associated with neonatal unconjugated bilirubin accumulation in *Ugt1*$^{-/-}$ mice could be prevented following the introduction of the human *UGT1* locus and the *UGT1A1* gene.[10] More recently, Muro's group generated another CN-I mouse model by inserting a premature stop codon in the *Ugt1a1* gene[11] and could thus prevent bilirubin-induced lethality with gene therapy. When they injected an adenovirus expressing human *UGT1A1* complementary DNA (cDNA), the neonatal mice reached adulthood with serum bilirubin levels similar to those in wild-type mice.[11] Although encouraging, gene therapy in humans is still in the experimental phases.

In the absence of functional UGT1A1, blockage of bilirubin production or accelerating alternative routes of bilirubin metabolism are the available choices to prevent the toxicity associated with SNH. To examine these choices, we assessed the impact of oxidative metabolism on bilirubin clearance and the potential of blocking bilirubin accumulation. In this study, we examined the potential of β-naphthoflavone and protoporphyrins (PPs) to block bilirubin accumulation. Due to the structural similarity between PPs and heme (Fig. 1), PPs have been exploited as HO-I inhibitors.[12] Following chemical treatment, bilirubin accumulation was assessed along with alterations in lethality.

Materials and Methods

ANIMALS AND CHEMICAL TREATMENTS

All mice used in the present study were housed under a 12-hour light/12-hour dark cycle at 21 °C-23 °C and received food and water *ad libitum*. Animal experiments were approved by the Animal Experimentation Committee of Kitasato University. The *Ugt1* knockout (KO) CN-I model mice as well as the *Tg (UGT1*^{A1}*28) Ugt1*$^{-/-}$ (humanized *UGT1* [*hUGT1*]) mice were developed previously in a C57BL/6 background.[9,10,13] Newborns were treated with zinc protoporphyrin (ZnPP, 1-100 µmol/kg/day, subcutaneously) from the second day after birth for 12 days. Blood was obtained from the submandibular vein and was then centrifuged at 3,000*g* for 5 minutes to obtain serum. Total serum bilirubin levels were quantified using a Bilirubinometer (B-105N; Erma, Tokyo, Japan). Mice were anesthetized by diethyl ether inhalation, and the livers were isolated and rinsed in cold 1.15% KCl and stored at −80 °C.

MICROARRAY AND GENE ONTOLOGY ANALYSIS

Livers from 2-day-old mice were used for microarray analysis. Heterozygous *Ugt1*$^{+/-}$ mice were bred to generate *Ugt1*$^{+/+}$, *Ugt1*$^{+/-}$, and *Ugt1*$^{-/-}$ (KO) mice. KO mice treated with ZnPP that matured to adults were further bred to produce *Ugt1*$^{-/-}$ (KOKO) mice. Three livers from each group (*Ugt1*$^{+/+}$, *Ugt1*$^{+/-}$, *KO*, and *KOKO*) were pooled. Total RNA was purified using a NucleoSpin RNA cleanup kit. RNA integrity was evaluated with a Nanodrop LITE Spectrophotometer. cDNA was synthesized from 500 ng of total RNA, amplified, fragmented, and labeled using a GeneChip WT PLUS Reagent kit according to the manufacturer's instructions. The biotinylated targets were hybridized to Mouse Gene 2.0 ST Array (Affymetrix, Santa Clara, CA) containing 35,240 transcripts. After hybridization, the arrays were washed and stained using a GeneChip Hybridization, Wash and Stain Kit according to the manufacturer's instructions. Afterward, the arrays were scanned with a GeneChip scanner 3000 7G (Affymetrix). GeneChip data quality control was performed using Expression Console Software, ver. 1.4, and raw data were preprocessed based on the Robust Multi-array Average algorithm for normalization and summarization.

Gene ontology (GO) analysis was conducted with a Cytoscape plugin BiNGO program.[14] GO analysis was also conducted using DAVID bioinformatics resources.[15]

QUANTITATIVE REVERSE-TRANSCRIPTION POLYMERASE CHAIN REACTION

Total RNA was extracted from tissues with Trizol reagent (Thermo Fisher Scientific, Waltham, MA). cDNA was synthesized from total RNA using ReverTra Ace (TOYOBO, Osaka, Japan) according to the manufacturer's protocol. Primers for mouse cyclophilin and human glyceraldehyde 3-phosphate dehydrogenase had been developed.[16,17] Sense and antisense oligonucleotide primers for mouse actin alpha-1 (5'-TCG CTG ACC GCA TGC A-3' and 5'-GGG CGA TGA TCT TGA TCT TCA-3') and human

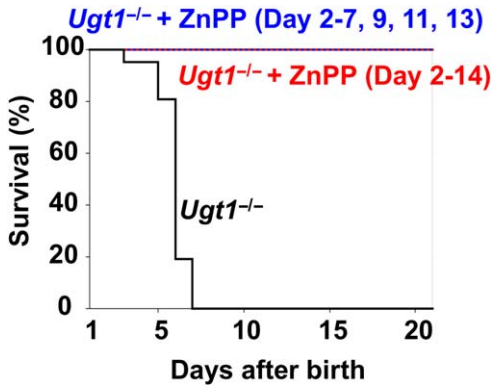

FIG. 2. Treatment of *Ugt1*$^{-/-}$ mice with ZnPP. Newborn *Ugt1*$^{-/-}$ mice were treated with ZnPP (100 μmol/kg/day, subcutaneously) from the second day after birth for 12 days, and their survival was monitored. The survival of chemical-treated mice is shown by the red line. The blue line indicates the survival of mice treated with ZnPP (100 μmol/kg/day) at days 2-7, 9, 11, and 13; n = 20 (*Ugt1*$^{-/-}$) and n = 10 (*Ugt1*$^{-/-}$ mice with ZnPP for both red and blue lines).

ACTIN alpha-1 (5'-CCC GCC CAG AAA CTA GAC AC-3' and 5'-GAC CCA TAC CGA CCA TGA CG-3') were established with the Primer Blast program (National Institutes of Health). Polymerase chain reaction conditions have been described.[18] Expression of cyclophilin and glyceraldehyde 3-phosphate dehydrogenase messenger RNA was used as an internal control for cDNA quantity and quality.

CELL CULTURE AND TREATMENTS

Human hepatoma HepG2 cells were obtained from DS Pharma Biomedical Co., Ltd. (Osaka, Japan). HepG2 cells were cultured as reported.[19] HepG2 cells were seeded at a density of 1×10^5/well in 12-well plates with the culture medium containing the indicated concentration (μM) of bilirubin and vitamin E (α-tocopherol). Twenty-four hours after incubation of the cells at 37 °C, total RNA was isolated from HepG2 cells using TRIzol reagent according to the manufacturer's instructions.

STATISTICS

Data were presented as means ± SD. Statistical analyses were conducted using the unpaired *t* test or Dunnett's test. A value of $P < 0.05$ was considered statistically significant.

Results

CHEMICAL TREATMENT OF CN-I MODEL MICE

Because there is no functional UGT1A1 in *Ugt1*$^{-/-}$ mice, these mice develop SNH with accumulation of bilirubin in brain tissue, which was identified as kernicterus. Due to the onset of kernicterus, SNH results in 100% fatality of newborn mice.[9] Although bilirubin is metabolized mainly through glucuronidation, it has been shown that oxidative metabolism by CYPs can also facilitate bilirubin metabolism. In our preliminary study, treatment of *Ugt1*$^{-/-}$ newborns with ß-naphthoflavone, an inducer of CYPs, slightly extended their survival (Supporting Fig. S1). Because HO-I is involved in the catabolism of heme, it was hypothesized that HO-I inhibitors could suppress the formation of bilirubin during the neonatal period and prevent the infiltration of bilirubin into the brain.[20] When *Ugt1*$^{-/-}$ mice were treated with low-dose ZnPP (1-10 μmol/kg/day) from 2 to 14 days after birth, none of the treated mice survived for more than 11 days. In contrast, *Ugt1*$^{-/-}$ mice survived when they were treated with ZnPP at a higher dosage (100 μmol/kg/day) (red line in Fig. 2). Serum bilirubin levels in the ZnPP-treated mice were less than 10.0 mg/dL at day 12, which was lower than the TSB levels in *hUGT1* mice at that same age (Fig. 3). Even though the chemical treatment was discontinued at 14 days after birth, the *Ugt1*$^{-/-}$ mice survived for more than

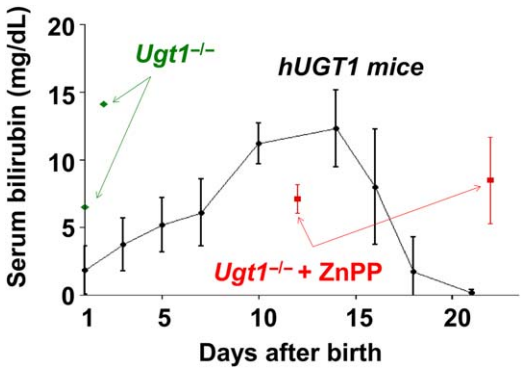

FIG. 3. Serum total bilirubin levels in hyperbilirubinemic mice. Blood was isolated from *Ugt1*$^{-/-}$ mice (green plots), *hUGT1* mice (black line), and *Ugt1*$^{-/-}$ mice treated with ZnPP, and bilirubin levels were determined; n = 25 (*hUGT1*), n = 6 (*Ugt1*$^{-/-}$), and n = 10 (*Ugt1*$^{-/-}$ with ZnPP). Data are mean ± SD.

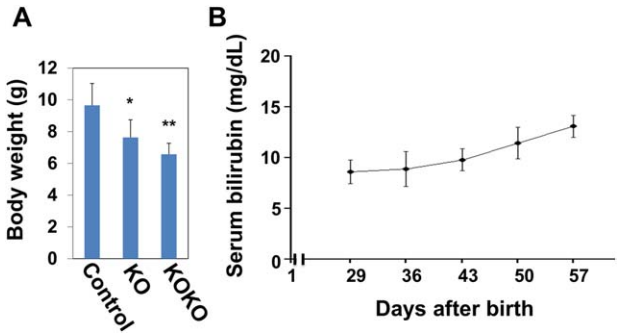

FIG. 4. Body weight and serum total bilirubin levels in *Ugt1*$^{-/-}$ mice. Neonatal *Ugt1*$^{-/-}$ mice were treated with ZnPP (Fig. 2). (A) Body weights of 22-day-old control mice, *Ugt1*$^{-/-}$ mice that were born from *Ugt1*$^{+/-}$ mice, and *Ugt1*$^{-/-}$ mice that were born from *Ugt1*$^{-/-}$ mice are shown. (B) Blood was isolated from the *Ugt1*$^{-/-}$ mice that were born from *Ugt1*$^{+/-}$ mice at 29, 36, 43, 50, and 57 days after birth, and bilirubin levels were determined. *, $P < 0.05$ and **, $P < 0.01$ in analysis of variance with post-hoc Tukey HSD test. n = 33 (control), n = 3 (KO mice), and n = 4 (KOKO mice) in panel A; n = 6 in panel B. Data are mean ± SD. KO and KOKO indicate *Ugt1*$^{-/-}$ mice that were born from *Ugt1*$^{+/-}$ female mice and *Ugt1*$^{-/-}$ mice that were born from *Ugt1*$^{-/-}$ female mice, respectively. Abbreviation: HSD, honest significant difference.

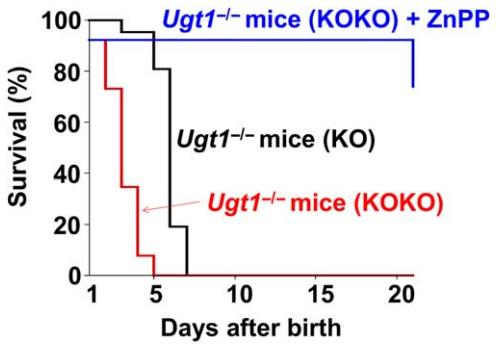

FIG. 5. Treatment of *Ugt1*$^{-/-}$ mice born from *Ugt1*$^{-/-}$ female mice with ZnPP. The survival curve of *Ugt1*$^{-/-}$ mice born from *Ugt1*$^{-/-}$ female mice (KOKO) is shown (red line) and is compared to that of *Ugt1*$^{-/-}$ mice born from *Ugt1*$^{+/-}$ female mice (KO) (black line). The *Ugt1*$^{-/-}$ mice born from *Ugt1*$^{-/-}$ female mice (KOKO) were treated with ZnPP (100 μmol/kg/day, subcutaneously) at days 2-14 after birth (blue line); n = 20 (black line), n = 10 (red line), and n = 5 (blue line).

21 days. When dosing entered the second week of treatment, ZnPP treatment (100 μmol/kg) could be administered every other day instead of every day (blue line in Fig. 2). At 22 days after birth, the mean TSB levels were 8.0 ± 3.0 mg/dL (Fig. 3).

ADULT CN-I MODEL MICE AND NEWBORNS FROM CN-1 MICE

Lethality associated with *Ugt1*$^{-/-}$ mice has been reported.[9,11] However, little is known about the phenotype of adult *Ugt1*$^{-/-}$ mice because the genotype is lethal. In our study, the administration of ZnPP to *Ugt1*$^{-/-}$ mice prevented neonatal lethality in a total of 20 *Ugt1*$^{-/-}$ mice (12 male, 8 female). Body weight of 22-day-old *Ugt1*$^{-/-}$ mice that were treated with ZnPP was 7.6 ± 1.1 g, which is lower than determined in same-age *Ugt1*$^{+/-}$ littermates (Fig. 4A). Body weight of *Ugt1*$^{-/-}$ mice gradually increased, and the weights of 2-month-old male and female *Ugt1*$^{-/-}$ mice were 22.3 ± 1.5 g and 20.5 ± 0.6 g, respectively, which is still lower than wild-type mice. When serum bilirubin levels were monitored, we found that the levels reached 13.4 ± 1.6 and 15.3 ± 2.3 mg/dL in 2-month-old male and female *Ugt1*$^{-/-}$ mice, respectively (Fig. 4B). Except for one male mouse, all the ZnPP-treated *Ugt1*$^{-/-}$ mice reached 2 months of age.

The successful treatment of *Ugt1*$^{-/-}$ mice with ZnPP to avoid SNH-induced lethality resulted in adult mice that could reproduce. Each delivery resulted in three to nine newborns per litter, and all were CN-I

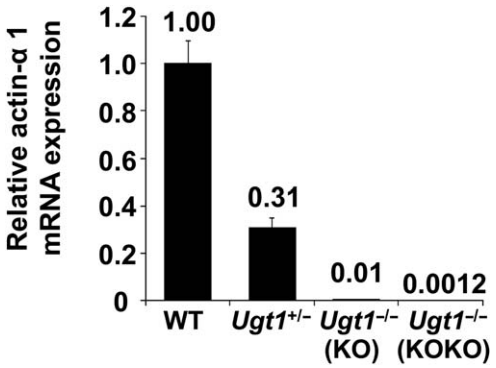

FIG. 6. Quantitative-PCR analysis of actin alpha-1 expression in the livers. Livers were isolated from 2-day-old WT mice, *Ugt1*$^{+/-}$ mice, *Ugt1*$^{-/-}$ mice that were born from *Ugt1*$^{+/-}$ female mice, and *Ugt1*$^{-/-}$ mice that were born from *Ugt1*$^{-/-}$ female mice (n = 3 each). Livers in each group were pooled, cDNA was synthesized, and expression levels of actin alpha-1 were determined by real-time PCR. Relative expression levels are shown in the figure. Data (mean ± SD) were pooled from five experiments. KO and KOKO indicate *Ugt1*$^{-/-}$ mice that were born from *Ugt1*$^{+/-}$ female mice and *Ugt1*$^{-/-}$ mice that were born from *Ugt1*$^{-/-}$ female mice, respectively. Abbreviations: mRNA, messenger RNA; PCR, polymerase chain reaction; WT, wild-type.

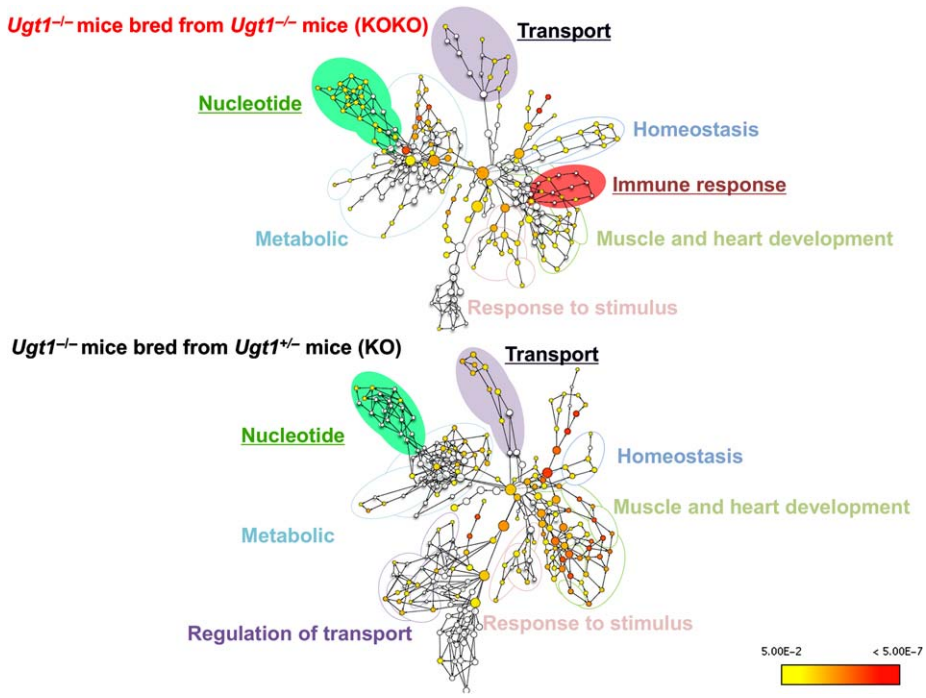

FIG. 7. GO analysis of down-regulated genes in hyperbilirubinemic mice. GO analysis of genes that were down-regulated in hyperbilirubinemia mice was conducted using a BiNGO program. KO and KOKO indicate $Ugt1^{-/-}$ mice that were born from $Ugt1^{+/-}$ female mice and $Ugt1^{-/-}$ mice that were born from $Ugt1^{-/-}$ female mice, respectively. Underlined groups, such as Transport, Nucleotide, and Immune Response, are categories that were specifically affected in $Ugt1^{-/-}$ mice.

as highlighted previously with the $Ugt1^{-/-}$ background. When we compared the survival curves of neonatal $Ugt1^{-/-}$ that were generated from crosses between $Ugt1^{+/-}$ male and female mice and crosses from ZnPP-treated male and female adult $Ugt1^{-/-}$ mice, the survival curve of offspring from ZnPP-treated mice was much shorter than from $Ugt1^{+/-}$ mice (Fig. 5, red line). Two days after birth, the TSB levels from neonatal $Ugt1^{-/-}$ mice generated from adult ZnPP-treated mice (14-15 mg/dL) were considerably higher than the newborns generated from $Ugt1^{+/-}$ breeders (2-10 mg/dL). We anticipate that the accelerated lethality was attributed to higher unconjugated bilirubin levels right after birth and was due to the incapability of bilirubin glucuronidation during pregnancy in the $Ugt1^{-/-}$ female mice.

TABLE 1. TOP 15 TRANSCRIPTS THAT WERE REDUCED IN THE LIVER OF $UGT1^{-/-}$ MICE (KOKO) IN MICROARRAY ANALYSIS

Cluster ID	Gene Symbol	Description	$Ugt1^{+/-}$	$Ugt1^{-/-}$ (KO)	$Ugt1^{-/-}$ (KOKO)
17513995	Acta1	actin, alpha 1, skeletal muscle	−3.79	−29.93	−36.18
17312186	Psca	prostate stem cell antigen	−41.83	−31.92	−28.79
17251133	Myh8	myosin, heavy polypeptide 8	−5.07	−26.96	−23.11
17318045	Cyp11b1	cytochrome P450, family 11, subfamily b1	−15.20	−18.95	−17.71
17517831	Cyp11a1	cytochrome P450, family 11, subfamily a1	−14.58	−15.91	−15.15
17322075	Krt4	keratin 4	−13.38	−12.95	−14.42
17343962	Cyp21a1	cytochrome P450, family 21, subfamily a1	−12.01	−11.27	−12.67
17517360	Sln	sarcolipin	−5.71	−15.29	−12.52
17223916	Myl1	myosin, light polypeptide 1	−3.30	−12.30	−11.95
17496211	Atp2a1	ATPase, Ca+ + transporting	−3.39	−13.47	−11.07
17290603	Actn2	actinin alpha 2	−3.41	−12.84	−10.34
17548055	LOC630751	interferon-inducible guanosine triphosphatase 1-like;	−3.66	−1.44	−9.50
17232453	Trdn	triadin	−3.67	−8.56	−8.62
17243910	Mybpc1	myosin binding protein C, slow-type	−3.32	−16.82	−8.61
17445565	Gm15611	predicted gene 15611	−1.92	−2.24	−8.41

Regardless, the newborns from the *Ugt1*$^{-/-}$ adults responded well to ZnPP treatment (blue line in Fig. 5) and reached adulthood. The body weight of 22-day-old *Ugt1*$^{-/-}$ mice generated from adult ZnPP-treated mice averaged 6.5 ± 0.7 g, which is significantly lower than wild-type mice (Fig. 4A).

MICROARRAY AND GO ANALYSIS OF NEWBORN *Ugt1*$^{-/-}$ MICE

The accelerated lethality that was apparent in the newborns from adult *Ugt1*$^{-/-}$ mice indicates that the elevated unconjugated bilirubin levels induce physiological toxicity that may include additional systemic processes in addition to those that are linked to the onset of chronic encephalopathy. To examine this possibility, we examined differences in liver gene expression in 2-day-old mice. The *Ugt1*$^{-/-}$ neonates generated from *Ugt1*$^{+/-}$ adult mice are referred to as KO mice, whereas the *Ugt1*$^{-/-}$ neonatal mice generated from adult (ZnPP-treated) *Ugt1*$^{-/-}$ mice are referred to as KOKO mice. When expression levels were determined, 598 genes with over a 2-fold change were observed, with 203 profiling as up-regulated and 395 being down-regulated. The quality of our microarray analysis was confirmed by quantitative polymerase chain reaction analysis of the *actin alpha-1* gene (Fig. 6). Because the number of genes and the fold changes were significantly greater with negatively regulated genes, we examined these transcripts and linked them through GO analysis (Fig. 7). Impressively, gene expression in KO and KOKO mice showed attenuated homeostatic processes affecting immune response, muscle contractility, transport processes, and metabolic function. From the list of the most significantly repressed genes (Table 1), such as those tied to muscle contraction (i.e., *Acta1, Myh8, My11*) and Ca^{2+} transport (i.e., *Sln, Atp2a1*), we can speculate that elevated TSB levels have a significant effect on cardiac function. Other key physiological processes as listed in the GO analysis (Table 2), such as key oxidative–reduction processes, support of the immune and inflammatory response, cholesterol metabolism, and downstream steroid production, were all compromised. Meanwhile, the number of genes and the fold changes were much less with positively regulated genes (Table 3). The GO mapping analysis further indicated that there was less impact of the positively regulated genes on biological processes (Fig. 8). Although the early actions of SNH in newborns have been shown to induce central nervous system toxicity, these studies indicate that

TABLE 2. GO ANALYSIS OF 395 TRANSCRIPTS THAT WERE DOWN-REGULATED IN THE LIVER

Category	Count	*P* Value
oxidation–reduction process	22	9.70E-04
immune response	14	8.70E-04
inflammatory response	14	1.90E-03
muscle contraction	13	5.30E-12
cellular response to interferon-gamma	13	2.50E-10
metabolic process	13	4.00E-02
cholesterol metabolic process	11	6.70E-07
positive regulation of guanosine triphosphatase activity	11	7.10E-05
positive regulation of extracellular signal-regulated kinase 1 and 2 cascade	11	5.30E-04
chemokine-mediated signaling pathway	10	1.30E-07
regulation of muscle contraction	9	7.40E-10
lymphocyte chemotaxis	9	3.00E-08
monocyte chemotaxis	9	1.40E-07
steroid biosynthetic process	9	3.10E-06
neutrophil chemotaxis	9	9.70E-06
cellular response to interleukin-1	9	3.60E-05
cellular response to tumor necrosis factor	9	2.20E-04
leukocyte chemotaxis	8	1.80E-08
negative regulation of myeloid cell differentiation	7	2.60E-06
steroid metabolic process	7	1.40E-03
sarcomere organization	6	7.90E-05
sodium ion transport	6	3.50E-02
mitophagy in response to mitochondrial depolarization	6	4.40E-02
skeletal muscle contraction	5	5.90E-04
defense response to protozoan	5	1.00E-03
cholesterol biosynthetic process	5	1.10E-03
cardiac muscle contraction	5	5.20E-03
skeletal muscle tissue development	5	1.30E-02
mesenchyme migration	4	3.00E-05
cellular response to follicle-stimulating hormone stimulus	4	7.80E-04
flavonoid glucuronidation	4	3.30E-03
flavonoid biosynthetic process	4	3.30E-03
sterol biosynthetic process	4	6.20E-03
skeletal muscle fiber development	4	6.90E-03
cellular response to interferon-beta	4	2.50E-02
C21-steroid hormone biosynthetic process	3	1.20E-03
skeletal muscle thin filament assembly	3	2.10E-03
regulation of striated muscle contraction	3	2.10E-03
sarcoplasmic reticulum calcium ion transport	3	3.00E-03
cardiac myofibril assembly	3	1.30E-02
regulation of cytoskeleton organization	3	2.00E-02
myofibril assembly	3	2.00E-02
positive regulation of T-cell migration	3	2.20E-02
regulation of release of sequestered calcium ion into cytosol by sarcoplasmic reticulum	3	2.50E-02
heart contraction	3	2.50E-02
intermediate filament organization	3	3.70E-02
negative regulation of dendritic cell dendrite assembly	2	2.90E-02
positive regulation of myeloid dendritic cell chemotaxis	2	2.90E-02
phosphocreatine metabolic process	2	2.90E-02
cellular response to growth hormone stimulus	2	2.90E-02
regulation of cell communication by electrical coupling	2	4.30E-02
cortisol metabolic process	2	4.30E-02
mesangial cell-matrix adhesion	2	4.30E-02

TABLE 3. TOP 15 TRANSCRIPTS THAT WERE INDUCED IN THE LIVER OF *UGT1*$^{-/-}$ (KOKO) IN THE MICROARRAY ANALYSIS

Cluster ID	Gene Symbol	Description	*Ugt1*$^{+/-}$	*Ugt1*$^{-/-}$ (KO)	*Ugt1*$^{-/-}$ (KOKO)
17307305	Phf11c	PHD finger protein 11C	3.03	1.01	10.38
17307318	Setdb2	SET domain, bifurcated 2	3.68	1.25	7.57
17441660	Sds	serine dehydratase	2.08	1.17	5.01
17280062	Lpin1	lipin 1	2.98	1.04	4.58
17368521			1.65	−1.13	3.94
17396238			1.14	1.62	3.91
17526707	Zbtb16	zinc finger and BTB domain containing 16	2.07	1.41	3.91
17370954	Upp2	uridine phosphorylase 2	1.38	−1.08	3.62
17236100			1.03	1.01	3.45
17312066			1.36	−1.13	3.45
17549958			1.03	1.01	3.45
17406186	Tdo2	tryptophan 2,3-dioxygenase	1.40	1.26	3.36
17364932	Got1	glutamate oxaloacetate transaminase 1	1.37	−1.01	3.26
17330168	BC100530	cDNA sequence BC100530	3.06	2.51	3.21
17370339	Olfr345	olfactory receptor 345	1.64	3.21	3.20

important systemic processes essential for neonatal development and overall health are influenced by early elevations in TSB immediately after birth.

REGULATION OF ACTIN-alpha 1 EXPRESSION IN HepG2 CELLS

Although bilirubin is neurotoxic, it is a potent antioxidant. To understand the involvement of antioxidant effects on the down-regulation of actin-alpha 1 expression in hepatic cells (Table 1; Fig. 6), human hepatoma HepG2 cells were treated with bilirubin and another antioxidant, vitamin E (α-tocopherol). In HepG2 cells, bilirubin concentration dependently reduced the expression of ACTIN α1 (Fig. 9A). A similar reduction in the expression of ACTIN-α1 was also observed in the α-tocopherol-treated HepG2 cells (Fig. 9B). These data strongly indicate that the expression of

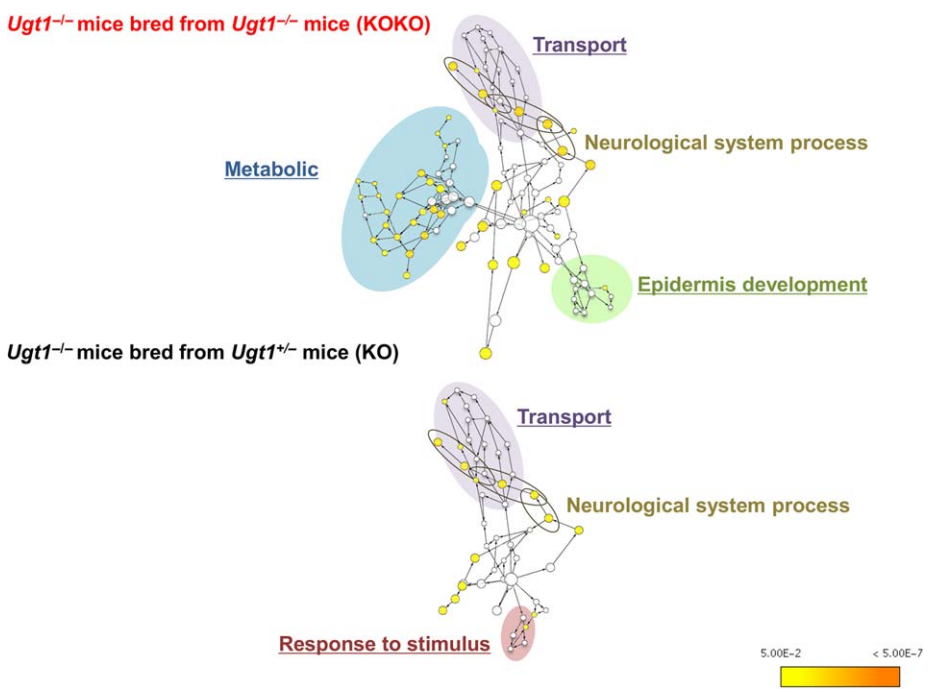

FIG. 8. GO analysis of up-regulated genes in hyperbilirubinemic mice. GO analysis of genes that were up-regulated in hyperbilirubinemia mice was conducted using a BiNGO program. KO and KOKO indicate *Ugt1*$^{-/-}$ mice that were born from *Ugt1*$^{+/-}$ female mice and *Ugt1*$^{-/-}$ mice that were born from *Ugt1*$^{-/-}$ female mice, respectively. Underlined groups, such as Transport and Metabolic, are categories that were specifically affected in *Ugt1*$^{-/-}$ mice.

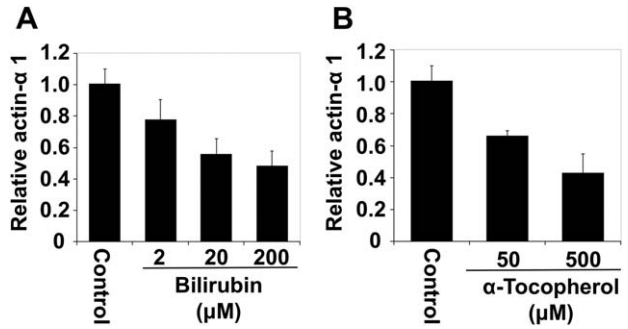

FIG. 9. Expression and regulation of ACTIN alpha-1 in chemical-treated HepG2 cells. HepG2 cells were treated with (A) bilirubin or (B) alpha-tocopherol with the indicated concentration for 24 hours. cDNA was synthesized, and expression levels of actin alpha-1 were determined by real-time PCR. Data are shown as mean ± SD (n = 5). Abbreviation: PCR, polymerase chain reaction.

hepatic actin-alpha 1 is regulated by the antioxidative property of bilirubin.

Discussion

Severe neonatal hyperbilirubinemia develops in newborns due to a dramatic imbalance in the production and UGT1A1-mediated metabolism of bilirubin. If untreated, escalating levels of TSB can lead to acute and chronic forms of encephalopathy, culminating in severe brain damage, which is classified as kernicterus. Chronic forms of bilirubin-induced encephalopathy can leave children with lifelong physical disabilities, including mental retardation.[21] Currently, there are no effective drug therapies to accelerate bilirubin metabolism or reduce bilirubin accumulation in cases of SNH. This is not a trivial clinical problem as this debilitating syndrome has been estimated to impact over 1 million children every year.[22] Thus, the implementation of effective animal models to study the impact of SNH on molecular and cellular processes targeted by elevated TSB levels can be effectively leveraged for the development of new therapeutics designed to prevent bilirubin toxicity.

An alternative approach to prevent the buildup of unconjugated bilirubin in CN1 is to block its initial accumulation by inhibiting HO-1, the initial rate-limiting step in bilirubin production. Metalloporphyrins, derivatives of heme, are effective inhibitors of HO-1 and have been tested in mice to examine their potential to decrease bilirubin production. ZnPP is a naturally occurring metalloporphyrin, a potent inhibitor of HO-1, and has been shown in mice preloaded with heme to inhibit liver HO-1 activity following intragastric injections.[23] Targeted deletion of the *Ugt1* locus in $Ugt1^{-/-}$ mice leads to newborn mice with nonhemolytic hyperbilirubinemia,[9] a condition that closely resembles CN-1 because there is no functional UGT1A1. Although the phenotype associated with the $Ugt1^{-/-}$ mice leads to rapid development of SNH, which is lethal within 1 week after birth,[9] we demonstrated that subcutaneous injections of ZnPP was effective in reducing TSB levels and preventing lethality (Fig. 2). In *hUGT1* mice that also develop SNH resulting from a developmental delay in UGT1A1 expression, induction of hemolysis by phenylhydrazine treatment to different-aged neonatal mice led to greater accumulation of TSB levels.[10] For the youngest age group (7-8-day old), 100% of the mice developed seizures and died compared to only 10% in 13-day-old mice. These findings indicated that SNH is a prelude to central nervous system (CNS) damage within the first 2 weeks of life, demonstrating that brain tissue maturation can combat the impact of bilirubin in later stages of development. By delaying the rapid accumulation of TSB levels in ZnPP-treated $Ugt1^{-/-}$ mice early in neonatal development, damaging levels of unconjugated bilirubin are not reached; maturation of brain tissue and the blood brain barrier then serve to block additional brain damage in the older mice. Thus, lowering TSB levels in this CN-1 model early in development protects brain tissue from damage, providing an opportunity to establish CNS defense against bilirubin toxicity.

Although the inability to metabolize bilirubin in newborns results in a clinical emergency, we have established the possibility that interrupting the production of bilirubin by blocking HO-1 activity may provide a unique mechanism for treating the most severe forms of hyperbilirubinemia. Once the appropriate dose of ZnPP was established for treating $Ugt1^{-/-}$ mice, we achieved nearly a 100% survival rate, with all the neonatal mice reaching adulthood (Fig. 2). Although their TSB levels plateaued around 10 mg/dL as adults (Fig. 4B), the $Ugt1^{-/-}$ mice showed no signs of bilirubin-induced toxicity and were capable of reproducing. However, compared to $Ugt1^{+/-}$ mice, adult $Ugt1^{-/-}$ mice weighed significantly less (Fig. 4A). This may indicate that bilirubin impacts insulin

sensitivity, which is directly correlated with obesity. For example, nonalcoholic fatty liver disease (NAFLD) is directly associated with obesity, insulin resistance, and metabolic syndrome.[24,25] Weight gain and the progression to NAFLD and the more severe form of nonalcoholic steatohepatitis have been linked to a mismatch between oxidative stress and decreased antioxidant capacity. In children and adolescents, bilirubin has been shown to be inversely associated with insulin resistance, the metabolic syndrome, and NAFLD.[26-28] These correlations between bilirubin accumulation against obesity and liver fibrosis may be due to the potent antioxidant properties associated with bilirubin.[29] In addition, it is well known that coronary artery disease can result from changes in serum lipid oxidation, an event that can be protected in individuals with higher TSB levels, such as those observed in Gilbert's syndrome. In the hyperbilirubinemic Gunn rat (j/j) model, adult mice at 24 weeks of age were 8% lighter than j/ + mice. When diabetes was induced by a single injection of streptozotocin, the j/j rats showed considerable resistance toward developing diabetes when compared to j/ + mice.[30] More recently, *hUGT1*28* mice, which express the human Gilbert's allele and show elevated TSB levels, accumulated less fat as adults with lower serum glucose and insulin levels.[31] These relationships indicate that elevated bilirubin levels in adult *Ugt1*$^{-/-}$ mice may provide homeostatic protection from diet-induced oxidative stress, which leads to changes in insulin and glucose production that directly impacts fat production. Furthermore, breast feeding has been known to be one of the factors increasing TSB in infants.[32-35] Breast milk-induced neonatal hyperbilirubinemia might be an essential condition for bringing beneficial advantages to the human body.

We have demonstrated that inhibition of HO-1 can be used to prevent lethality associated with SNH in newborn *Ugt1*$^{-/-}$ mice. Although CNS toxicity in SNH is known as the primary damage in humans and replicable animal models, evidence is presented that systemic toxicities other than brain damage may be contributing to the irreversible damage that occurs in cases of extreme SNH shortly after birth. In line with epidemiologic studies in humans and corroborated in animal studies, hyperbilirubinemia in adults may be preventing diet-induced oxidative stress and its negative effect on weight gain, providing additional clues that hyperbilirubinemia can protect against the deleterious actions of insulin and glucose insensitivity. These studies may provide an opportunity to advance the development of effective therapeutics to rapidly and effectively prevent bilirubin-induced toxicities. In addition, an improved understanding of the underlying benefits of hyperbilirubinemia and the mechanisms leading to a reduction in diet-induced oxidative stress can be pursued.

Acknowledgment: We are grateful to Dr. Yoshihiro Maruo (Shiga University of Medical Science) for critically reviewing this manuscript.

REFERENCES

1) Tenhunen R, Marver HS, Schmid R. Microsomal heme oxygenase. Characterization of the enzyme. J Biol Chem 1969;244:6388-6394.
2) Baranano DE, Rao M, Ferris CD, Snyder SH. Biliverdin reductase: a major physiologic cytoprotectant. Proc Natl Acad Sci U S A 2002;99:16093-16098.
3) Sedlak TW, Snyder SH. Bilirubin benefits: cellular protection by a biliverdin reductase antioxidant cycle. Pediatrics 2004;113:1776-1782.
4) Bosma PJ, Chowdhury JR, Bakker C, Gantla S, de Boer A, Oostra BA, et al. The genetic basis of the reduced expression of bilirubin UDP-glucuronosyltransferase 1 in Gilbert's syndrome. N Engl J Med. 1995;333:1171-1175.
5) Kapitulnik J, Gonzalez FJ. Marked endogenous activation of the CYP1A1 and CYP1A2 genes in the congenitally jaundiced Gunn rat. Mol Pharmacol. 1993;43:722-725.
6) Fujiwara R, Maruo Y, Chen S, Tukey RH. Role of extrahepatic UDP-glucuronosyltransferase 1A1: Advances in understanding breast milk-induced neonatal hyperbilirubinemia. Toxicol Appl Pharmacol 2015;289:124-132.
7) Bosma PJ, Chowdhury NR, Goldhoorn BG, Hofker MH, Oude Elferink RP, Jansen PL, et al. Sequence of exons and the flanking regions of human bilirubin-UDP-glucuronosyltransferase gene complex and identification of a genetic mutation in a patient with Crigler-Najjar syndrome, type I. Hepatology. 1992;15:941-947.
8) Cashore WJ. The neurotoxicity of bilirubin. Clin Perinatol. 1990;17:437-447.
9) Nguyen N, Bonzo JA, Chen S, Chouinard S, Kelner MJ, Hardiman G, et al. Disruption of the ugt1 locus in mice resembles human Crigler-Najjar type I disease. J Biol Chem 2008;283:7901-7911.
10) Fujiwara R, Nguyen N, Chen S, Tukey RH. Developmental hyperbilirubinemia and CNS toxicity in mice humanized with the UDP glucuronosyltransferase 1 (UGT1) locus. Proc Natl Acad Sci U S A 2010;107:5024-5029.
11) Bortolussi G, Zentilin L, Baj G, Giraudi P, Bellarosa C, Giacca M, et al. Rescue of bilirubin-induced neonatal lethality in a mouse model of Crigler-Najjar syndrome type I by AAV9-mediated gene transfer. FASEB J 2012;26:1052-1063.
12) Sahoo SK, Sawa T, Fang J, Tanaka S, Miyamoto Y, Akaike T, et al. Pegylated zinc protoporphyrin: a water-soluble heme oxygenase inhibitor with tumor-targeting capacity. Bioconjug Chem 2002;13:1031-1038.
13) Chen S, Beaton D, Nguyen N, Senekeo-Effenberger K, Brace-Sinnokrak E, Argikar U, et al. Tissue-specific, inducible, and

hormonal control of the human UDP-glucuronosyltransferase-1 (UGT1) locus. J Biol Chem 2005;280:37547-37557.
14) Maere S, Heymans K, Kuiper M. BiNGO: a Cytoscape plugin to assess overrepresentation of gene ontology categories in biological networks. Bioinformatics 2005;21:3448-3449.
15) **Huang da W**, **Sherman BT**, Lempicki RA. Systematic and integrative analysis of large gene lists using DAVID bioinformatics resources. Nat Protoc 2009;4:44-57.
16) Kutsuno Y, Hirashima R, Sakamoto M, Ushikubo H, Michimae H, Itoh T, et al. Expression of UDP-glucuronosyltransferase 1 (UGT1) and glucuronidation activity toward endogenous substances in humanized UGT1 mouse brain. Drug Metab Dispos 2015;43:1071-1076.
17) Fujiwara R, Takenaka S, Hashimoto M, Narawa T, Itoh T. Expression of human solute carrier family transporters in skin: possible contributor to drug-induced skin disorders. Sci Rep 2014;4:5251.
18) Hirashima R, Michimae H, Takemoto H, Sasaki A, Kobayashi Y, Itoh T, et al. Induction of the UDP-glucuronosyltransferase 1A1 during the perinatal period can cause neurodevelopmental toxicity. Mol Pharmacol 2016;90:265-274.
19) Asakura M, Karaki F, Fujii H, Atsuda K, Itoh T, Fujiwara R. Vildagliptin and its metabolite M20.7 induce the expression of S100A8 and S100A9 in human hepatoma HepG2 and leukemia HL-60 cells. Sci Rep 2016;6:35633.
20) Drummond GS, Kappas A. Sn-protoporphyrin inhibition of fetal and neonatal brain heme oxygenase. Transplacental passage of the metalloporphyrin and prenatal suppression of hyperbilirubinemia in the newborn animal. J Clin Invest. 1986;77:971-976.
21) Bhutani VK, Johnson-Hamerman L. The clinical syndrome of bilirubin-induced neurologic dysfunction. Semin Fetal Neonatal Med 2015;20:6-13.
22) Bhutani VK, Zipursky A, Blencowe H, Khanna R, Sgro M, Ebbesen F, et al. Neonatal hyperbilirubinemia and Rhesus disease of the newborn: incidence and impairment estimates for 2010 at regional and global levels. Pediatr Res 2013;74(Suppl. 1):86-100.
23) Fujioka K, Kalish F, Wong RJ, Stevenson DK. Inhibition of heme oxygenase activity using a microparticle formulation of zinc protoporphyrin in an acute hemolytic newborn mouse model. Pediatr Res 2016;79:251-257.
24) Seki E, Brenner DA. Recent advancement of molecular mechanisms of liver fibrosis. J Hepatobiliary Pancreat Sci 2015;22:512-518.
25) Cusi K. Role of obesity and lipotoxicity in the development of nonalcoholic steatohepatitis: pathophysiology and clinical implications. Gastroenterology 2012;142:711-725.
26) Lin LY, Kuo HK, Hwang JJ, Lai LP, Chiang FT, Tseng CD, et al. Serum bilirubin is inversely associated with insulin resistance and metabolic syndrome among children and adolescents. Atherosclerosis 2009;203:563-568.
27) Puri K, Nobili V, Melville K, Corte CD, Sartorelli MR, Lopez R, et al. Serum bilirubin level is inversely associated with nonalcoholic steatohepatitis in children. J Pediatr Gastroenterol Nutr 2013;57:114-118.
28) Jenko-Praznikar Z, Petelin A, Jurdana M, Žiberna L. Serum bilirubin levels are lower in overweight asymptomatic middle-aged adults: an early indicator of metabolic syndrome? Metabolism 2013;62:976-985.
29) Vitek L. The role of bilirubin in diabetes, metabolic syndrome, and cardiovascular diseases. Front Pharmacol 2012;3:55.
30) Fujii M, Inoguchi T, Sasaki S, Maeda Y, Zheng J, Kobayashi K, et al. Bilirubin and biliverdin protect rodents against diabetic nephropathy by downregulating NAD(P)H oxidase. Kidney Int 2010;78:905-919.
31) Hinds TD Jr, Hosick PA, Chen S, Tukey RH, Hankins MW, Nestor-Kalinoski A, et al. Mice with hyperbilirubinemia due to Gilbert's Syndrome polymorphism are resistant to hepatic steatosis by decreased serine 73 phosphorylation of PPARalpha. Am J Physiol Endocrinol Metab 2017;312:E244-E252.
32) Huang MJ, Kua KE, Teng HC, Tang KS, Weng HW, Huang CS. Risk factors for severe hyperbilirubinemia in neonates. Pediatr Res 2004;56:682-689.
33) Fujiwara R, Chen S, Karin M, Tukey RH. Reduced expression of UGT1A1 in intestines of humanized UGT1 mice via inactivation of NF-κB leads to hyperbilirubinemia. Gastroenterology 2012;142:109-118.e2.
34) Shibuya A, Itoh T, Tukey RH, Fujiwara R. Impact of fatty acids on human UDP-glucuronosyltransferase 1A1 activity and its expression in neonatal hyperbilirubinemia. Sci Rep 2013;3:2903.
35) Aoshima N, Fujie Y, Itoh T, Tukey RH, Fujiwara R. Glucose induces intestinal human UDP-glucuronosyltransferase (UGT) 1A1 to prevent neonatal hyperbilirubinemia. Sci Rep 2014;4:6343.

Author names in bold designate shared co-first authorship.

Supporting Information

Additional Supporting Information may be found at onlinelibrary.wiley.com/doi/10.1002/hep4.1082/full.